Electronic Supplementary Information of

An electrochemical sensor based on AuPd@Fe_xO_y nanozyme for sensitive and in-situ quantitative detection of hydrogen peroxide in real samples

Mengjiao Dai [a,b], *Qunyan Zhu* [a *], *Dongxue Han* [d], *Li Niu* [d], *Zhenxin Wang* [a,b,c *]

[a]State Key Laboratory of Electroanalytical Chemistry, Changchun Institute of Applied Chemistry, Chinese Academy of Sciences, Changchun 130022, Jilin, China.

[b]University of Science and Technology of China, Hefei 230026, China.

[c]National Analytical Research Center of Electrochemistry and Spectroscopy, Changchun Institute of Applied Chemistry, Chinese Academy of Sciences, Changchun 130022, Jilin, China.

[d]Center for Advanced Analytical Science, c/o School of Chemistry and Chemical Engineering, Guangzhou University, Guangzhou 510006, P.R. China.

* Corresponding Authors：

E-mail: wangzx@ciac.ac.cn (ZW); Tel: +86-431-85262243；

E-mail: zhuqy@ciac.ac.cn. (QZ)

Table of Contents

1. Additional Experimental Section

1.1 Reagents. $HAuCl_4$, Na_2PdCl_4, Nafion117 solution (Nafion, 5%) and N-Formyl-L-methionyl-L-leucyl-L-phenylalanine (fMLP, 97%) were obtained from Sigma-Aldrich CO. (MO, USA). $FeCl_2$, penicillin and streptomycin were obtained from Aladdin Reagent CO., Ltd. (Shanghai, China). The high glucose Dulbecco's Modified Eagle Medium (DMEM), Fetal bovine serum (FBS) trypsin-EDTA cell detaching kit were purchased from Gibco Co. (New York, USA). MCF-7 cell lines were purchased from Shanghai Cell Bank, CAS (Shanghai, China). The other reagents were obtained from Beijing Chemical Reagents Co. (Beijing China). All chemicals were analytical grade and used as received without further purification. Phosphate buffered saline (PBS, 10 mM, pH 7.4, NaCl 137 mM) was used in all experiments. Milli-Q water (18.2 MΩ cm) was used throughout. Disinfectant was purchased from Hebei Jianning Medical Chemical Plant (Hebei, China).

1.2 Instruments. The TECNAI G2 high-resolution transmission electron microscope was used to get Transmission electron microscope (TEM) images. Zeta potential measurements were carried out on Malvern Zetasizer (Malvern Instrument Ltd, UK). The scanning electronic microscopy (SEM) micrographs were recorded on a Gemini SEM 300 scanning electron microscope (ZEISS, Germany) at an acceleration voltage of 15.0 kV. The information about the element composition of the electrode surface was investigated by SEM coupled with energy-dispersive X-ray spectroscopy (EDX). SEM-mapping images were obtained by SEM coupled with an ULTIM MAX (Oxford Instruments, UK) silicon drift detector. The metal contents of the sample were measured by ICP–MS, on a Thermo Scientific iCAP TQ (Thermo Fisher Scientific, USA). UV-vis spectra of oxidized TMB was monitored by using PowerWave XS2 microplate reader (BioTek Instruments, Inc., USA). Cells are counted by Cellometer Mini Cell Counter (Nexcelom Bioscience LLC, USA). The differential pulse voltammetry (DPV), amperometric measurements and Electrochemical impedance spectroscopy (EIS) were performed on a CHI 660D electrochemical workstation (Shanghai CH Instrument Ltd., China).

1.3 Synthesis of AuPd@Fe_xO_y NPs. 2.5 mL of $HAuCl_4$ (0.024 M) and 2.5 mL of

Na_2PdCl_4 (0.024 M) were added into 500 mL of ultrapure water. Under continuous stirring, 25 mL of ammonia solution (0.075%) was rapidly added into the mixture solution at room temperature. After stirring for 2 min, 15 mL of $FeCl_2$ aqueous solution (0.1 M) was rapidly added and continuous stirring for 20 min. The products were collected by centrifugation (8500 rpm, 10 min) and washed by water for three times. Then, the as-prepared AuPd@Fe_xO_y NPs was dispersed in aqueous solution for further use.

1.4 Evaluating the peroxidase-mimicking activity of AuPd@Fe_xO_y NPs. The apparent kinetic parameters of K_m and V_{max} were obtained by the Michaelis-Menten equation and Lineweaver-Burk plot (as shown in following equations 1 and 2), respectively.

$$V = V_{max} \times [H_2O_2]/(K_m + [H_2O_2]) \quad (1)$$

$$1/V = (K_m/V_{max}) \times (1/[H_2O_2]) + 1/V_{max} \quad (2)$$

The V_{max} refers to apparent maximum initial velocity, K_m refers to apparent Michaelis-Menten constant, V refers to initial velocity, and $[H_2O_2]$ refers to the concentration of substrate.

For peroxidase-like activity assays, UV-visible spectra of 200 μL mixture contained 1.0 mM TMB and 4.78 μg/mL AuPd@Fe_xO_y NPs (calculated *via* [Fe]), and various concentrations of H_2O_2 (from 1.0 to 50 mM) were recorded (n=3). The maximum absorbance at 652 nm (OD_{652}) were used to calculate the K_m and V_{max}.

1.5 Electrochemical impedance spectroscopy. Electrochemical impedance spectroscopy (EIS) was performed in 8 mL solution containing 0.1 M KCl and 5 mM $K_3[Fe(CN)_6]$ and 5 mM $K_4[Fe(CN)_6]$ with the frequency range of 1 to 10^6 Hz.

1.6 The electrocatalytic mechanism of AuPd@Fe_xO_y NPs.

The Fe element of AuPd@Fe_xO_y NPs in the AuPd@Fe_xO_y/GCE acts as catalyst for H_2O_2.

Electrochemical cathodic (the working electrode) reaction at -0.20 V (as shown in following equations 3 and 4):

$$2Fe^{3+} + 2e^- \rightarrow 2Fe^{2+} \quad (3)$$

$$2Fe^{2+} + H_2O_2 + 2H^+ \rightarrow 2Fe^{3+} + 2H_2O \quad (4)$$

1.7 Analysis of disinfectant. The disinfectant was diluted 1000-folds by 10 mM PBS as sample solution. Then, 500 μM, 1000 μM, 1500 μM of H_2O_2 were spiked into the sample solution for DPV measurements, respectively. Each measurement was repeated three times.

1.8 The static state chronoamperometry measurement. The static state chronoamperometry measurements were conducted in a standard three-electrode cell. The AuPd@Fe_xO_y NPs/GCE, Ag/AgCl electrode, and Pt disk electrode were used as the working electrode, reference electrode, and counter electrode, respectively. 3 mL of PBS were added into a well of 12-well plates for EC sensing. After the background noise was stabilized, the chronoamperometry measurement was paused, and different concentrations H_2O_2 were injected into the well. After gently shaking for 10 seconds and standing for 1 minute, the corresponding current responses were recorded.

2. Additional Figures

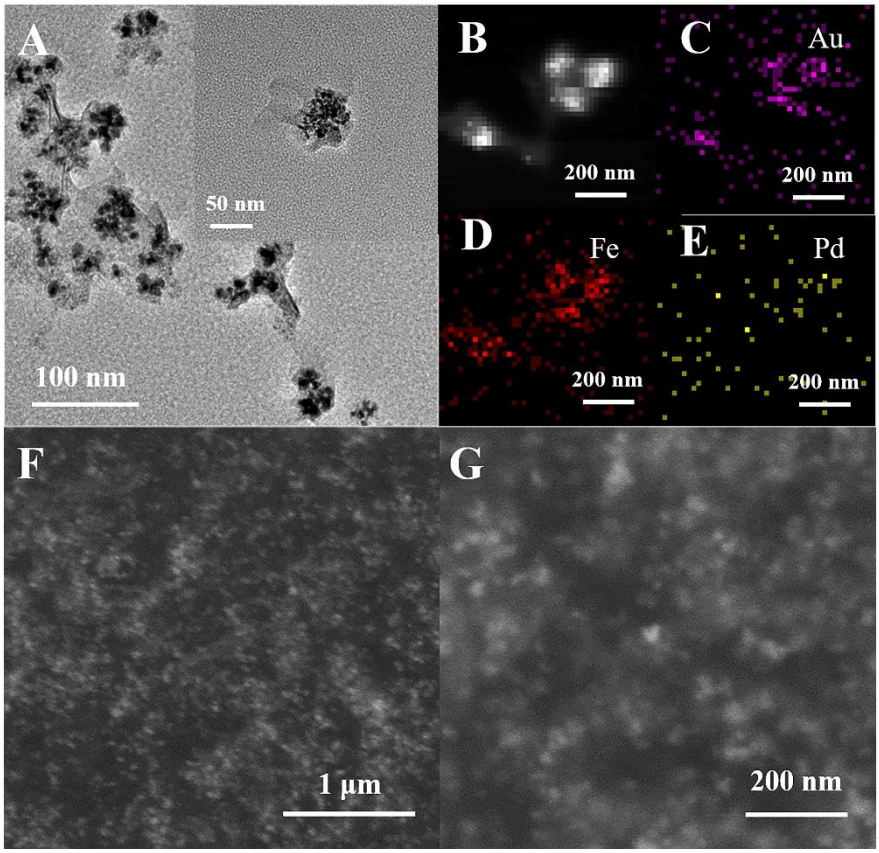

Fig. S1 (A) The TEM micrographs of AuPd@Fe_xO_y NPs with low and high (the inset) magnification, respectively; (B–E) HAADF-STEM micrograph and corresponding elemental mapping of Au, Fe and Pd of AuPd@Fe_xO_y NPs, respectively; (F) and (G) SEM micrographs of AuPd@Fe_xO_y NPs/GCE with low and high magnification.

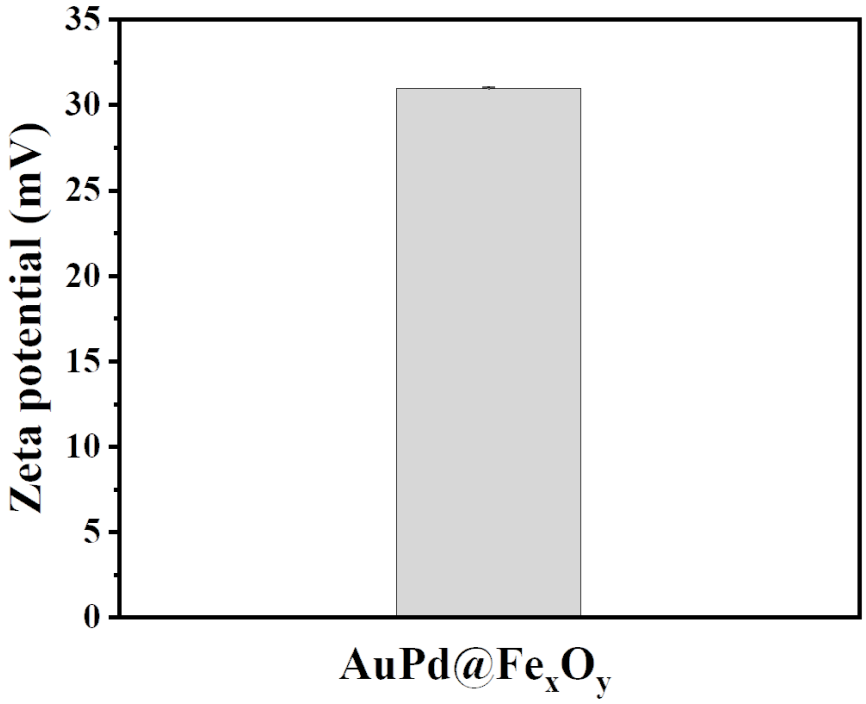

Fig. S2 Zeta potential of AuPd@Fe_xO_y NPs (n = 3).

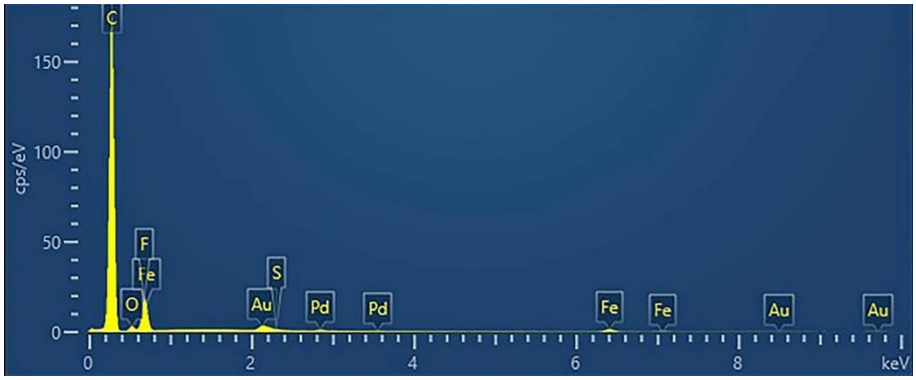

Fig. S3 EDX analysis of AuPd@Fe_xO_y NPs/GCE.

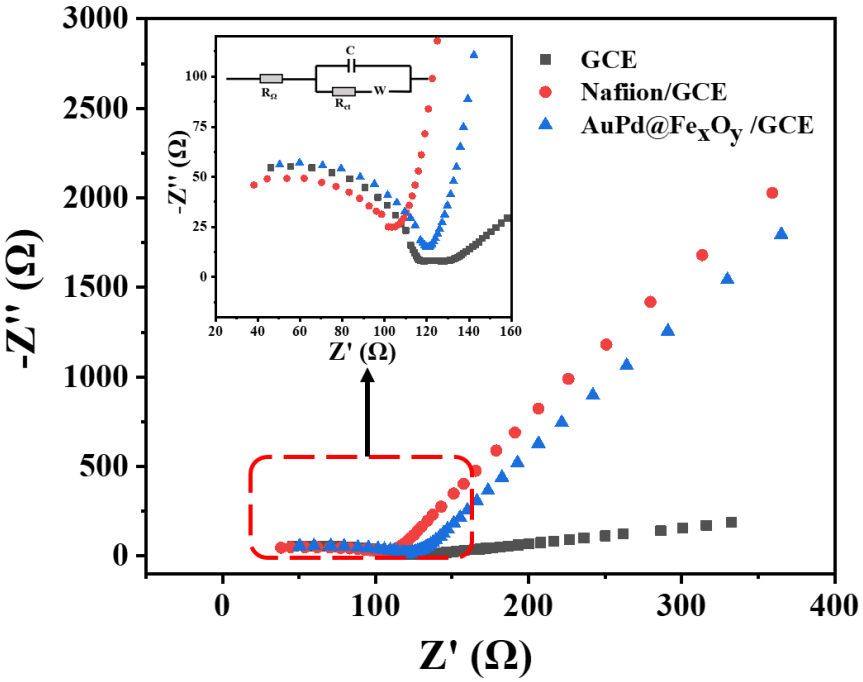

Fig. S4 Nyquist diagrams recorded at bare GCE, Nafion/GCE and AuPd@Fe_xO_y NPs/GCE in a solution containing 0.1 M KCl and 5 mM $Fe(CN)_6^{3-}/Fe(CN)_6^{4-}$ with a frequency range of 1 to 10^6 Hz. The inset shows that the equivalent circuit used to fit the Nyquist plots obtained from modified electrodes. R_Ω and R_{ct} represent electrolyte resistance and charge transfer resistance; C is the double layer capacitance; W corresponds to Warburg impedance.

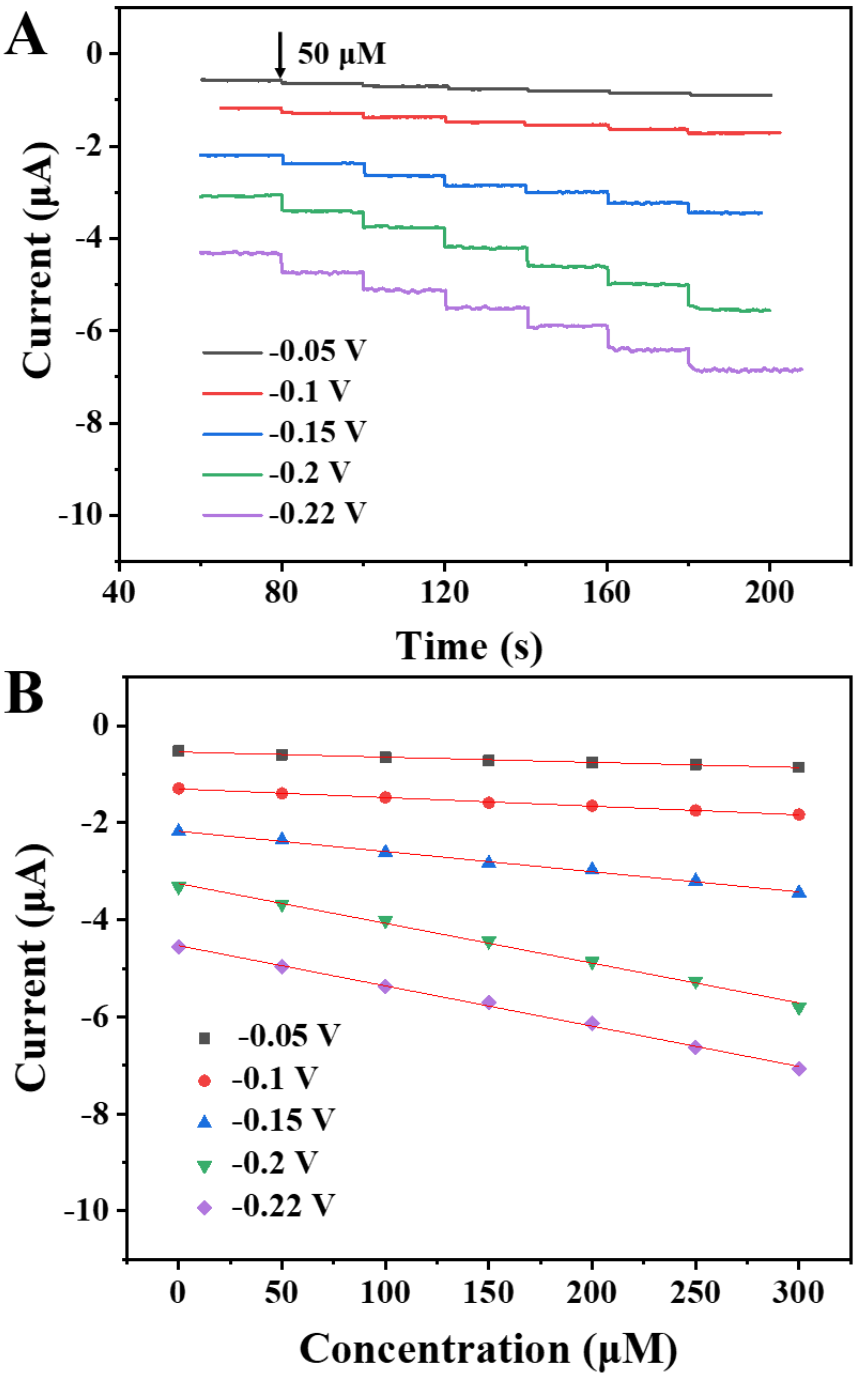

Fig. S5 (A) The amperometric response curves of AuPd@Fe_xO_y NPs/GCE in 10 mM of PBS with successively adding of H_2O_2 at different applied potentials, (B) the corresponding current response as a function of the concentration of H_2O_2.

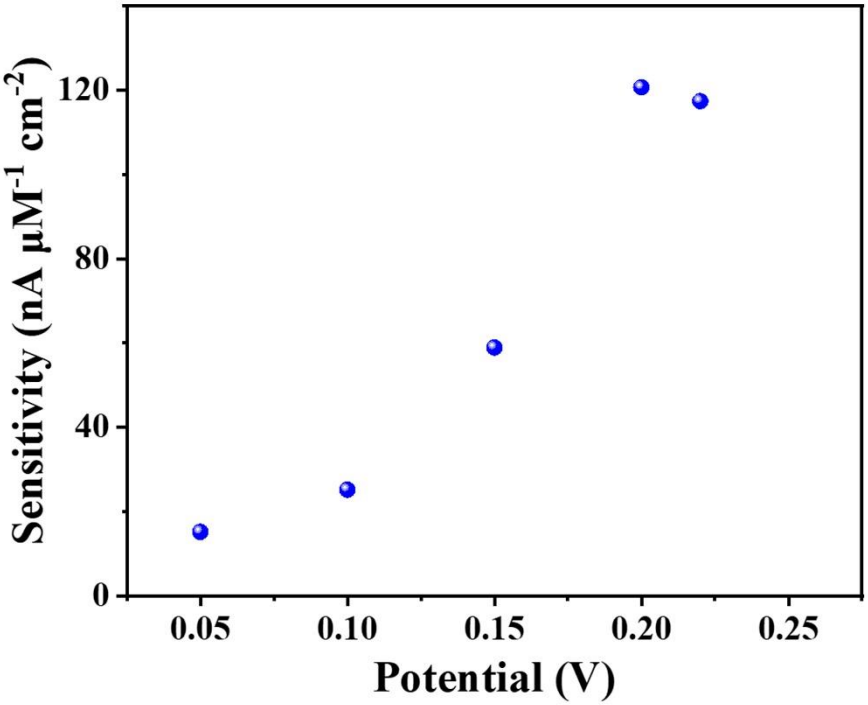

Fig. S6 The sensitivity values of AuPd@Fe_xO_y NPs/GCE in 10 mM of PBS with successively adding of H_2O_2 at different applied potentials.

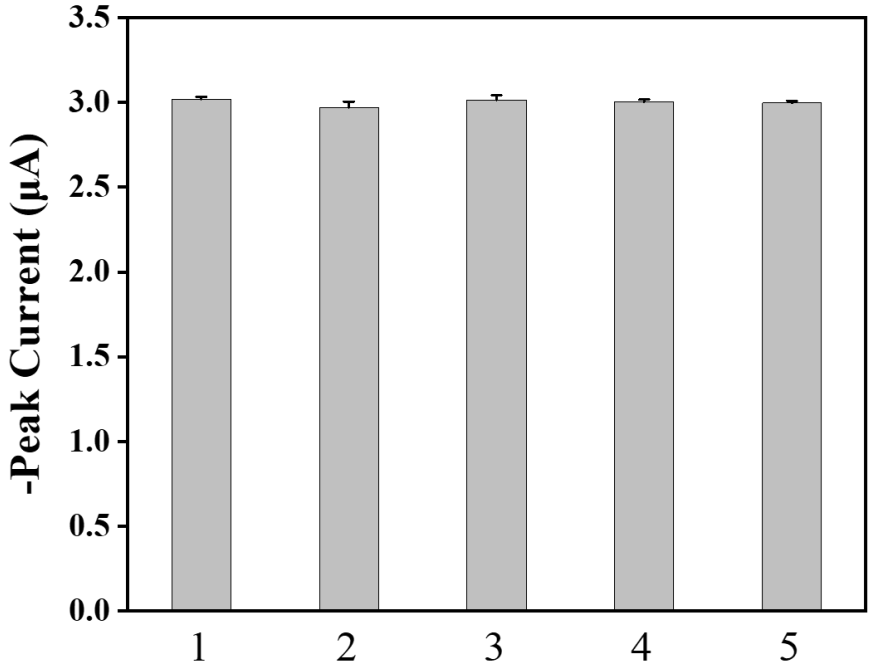

Fig. S7 The DPV peak currents in 500 μM M H_2O_2 of five AuPd@Fe_xO_y NPs/GCEs from five batches (n=3).

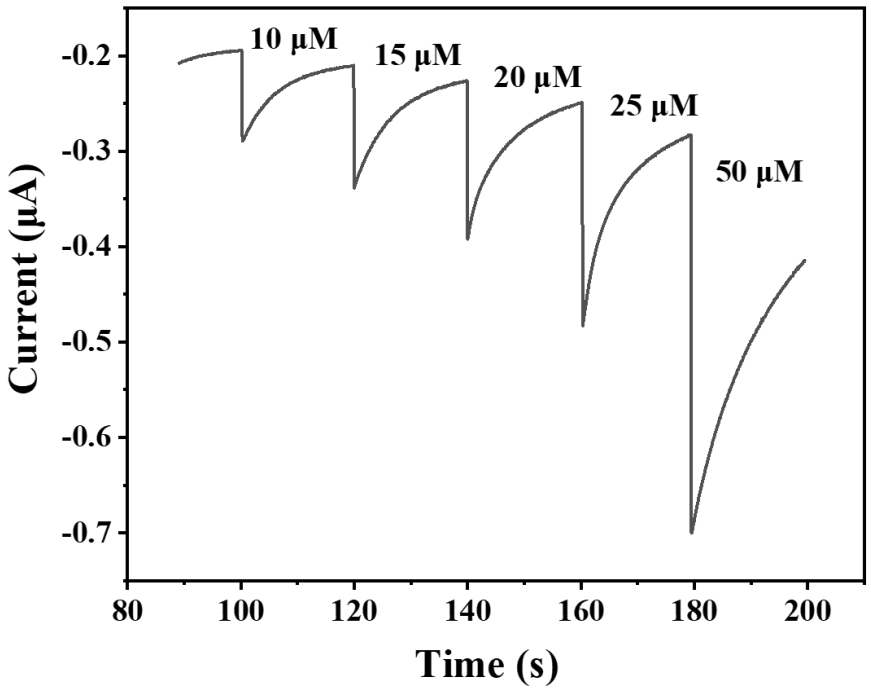

Fig. S8 The static state chronoamperometric responses of AuPd@Fe_xO_y NPs/GCE in various concentrations of H_2O_2.

3. Additional Tables

Table S1 The elemental composition distribution of AuPd@Fe_xO_y/GCE sensor

Element	Line type	Wt%	At%
C	K	79.93	89.05
O	K	2.78	2.32
F	K	10.49	7.39
S	K	0.20	0.08
Fe	K	3.95	0.95
Pd	L	0.47	0.06
Au	M	2.19	0.15
Total		100.00	100.00

Table S2 Comparison of the analytical performance of AuPd@Fe_xO_y NPs/GCE with those of non-enzymatic-based H_2O_2 electrochemical sensors reported by literature

Electrode materials	Measurements	Linear range (μM)	Limit of detection (μM)	Sensitivity (μA cm^{-2} mM^{-1})	Reference
Inkjet printing Ag	Chronoamperometry	100–6800	5.0	287	[S1]
Cr-MOF (MIL-53-Cr^{III})	DPV	25–500	3.52	–	[S2]
SeNPs-FTO	Chronoamperometry	100–20000	79.3	104.2	[S3]
m-MoS_2@CNS	Chronoamperometry	100–20000	7.5	8.89	[S4]
PtNPs-SeNPs-FTO	Chronoamperometry	10–40000	5	7.3	[S5]
MoS_2-ICPC	Chronoamperometry	20–300	11.8	–	[S6]
AuPd@Fe_xO_y	DPV	13–6000	1.6	83.8	**This work**
	Chronoamperometry	50–1000	3.0	120.7	

Table S3 Comparison of the current changes of static state chronoamperometric response (ΔI_s) in various concentrations of H_2O_2 with those calculated by calibration curve Fig. 4D (multiplying concentration of H_2O_2 with the lope of calibration curve (8.53 nA μM^{-1}) gains standard chronoamperometric response (ΔI_0))

Concentration (μM)	$-\Delta I_s$ (nA)	$-\Delta I_0$ (nA)	$\Delta I_s/\Delta I_0$ (%)
10	87.4	85.3	102.4
15	128.3	128.0	100.2
20	165.9	170.6	97.2
25	233.8	213.3	109.6
50	416.9	426.5	97.8

4. Additional References

[S1] L. Shi, M. Layani, X. Cai, H. Zhao, S. Magdassi, M. Lan, An inkjet printed Ag electrode fabricated on plastic substrate with a chemical sintering approach for the electrochemical sensing of hydrogen peroxide, Sensors and Actuators B: Chemical 256 (2018) 938-945.

[S2] N.S. Lopa, M.M. Rahman, F. Ahmed, S. C. Sutradhar, T. Ryu, W. Kim, A base-stable metal-organic framework for sensitive and non-enzymatic electrochemical detection of hydrogen peroxide, Electrochimica Acta 274 (2018) 49-56.

[S3] N.S. Dumore, M. Mukhopadhyay, Sensitivity enhanced SeNPs-FTO electrochemical sensor for hydrogen peroxide detection, Journal of Electroanalytical Chemistry 878 (2020) 114544.

[S4] I.W. Cho, S.U. Son, M. Yang, J. Choi, Preparation of microporous MoS_2@carbon nanospheres for the electrochemical detection of hydrogen peroxide, Journal of Electroanalytical Chemistry 876 (2020)114739.

[S5] N.S. Dumore, M. Mukhopadhyay, Development of novel electrochemical sensor based on PtNPs-SeNPs-FTO nanocomposites via electrochemical deposition for detection of hydrogen peroxide, Journal of Environmental Chemical Engineering 10 (2022) 107058.

[S6] S. Mutyala, J. Kinsly, G.V.R. Sharma, S. Chinnathambi, M. Jayaraman, Non-enzymatic electrochemical hydrogen peroxide detection using MoS_2- Interconnected porous carbon heterostructure, Journal of Electroanalytical Chemistry 823 (2018) 429-436.